Science Advances
AAAS

Supplementary Materials for

Mechanical regulation of talin through binding and history-dependent unfolding

Narayan Dahal *et al.*

Corresponding author: Ionel Popa, popa@uwm.edu

Sci. Adv. **8**, eabl7719 (2022)
DOI: 10.1126/sciadv.abl7719

This PDF file includes:

Supplementary Tables:

Supplementary Table 1. Binding sites for talin domains

Domain Name	Binding Partners
F0	Rap1
F1	PIP2
F2	Actin, PIP2
F3	Actin, β-Integrin, RIAM, PIP2, FAK, TIAM1, Layilin, PIP1γ90, Gα13, R9
R1	Vinculin
R2	Vinculin x2, RIAM
R3	Vinculin x2, RIAM
R4	Actin
R5	Actin
R6	Vinculin, Actin
R7	Vinculin, Actin, KANK1, α-Synemin
R8	Vinculin, Actin, RIAM, DLC1, Paxillin, α-Synemin, CDK1
R9	F3
R10	Vinculin, calpain
R11	Vinculin, RIAM, β-Integrin, Moesin
R12	β-Integrin, Moesin
R13	Vinculin, Actin, Moesin
DD	Actin, DD

Compiled from References (*10, 19, 50-54*)

Supplementary Table 2. Expected number of amino acids from unfolding of various intermediates in the R7R8 structure.

Structure	Number of aa	Structure	Number of aa
R7R8	294	R7(H4&H5)	72
R7 full length	176	R7(H1&H5)	60
R7(H2-H5)	147	R8 full length	118
R7(H2-H4)	116	R8 (H1'&H4')	59
R7(H1-H3)	104	R8 (H4')	34

Supplementary Table 3. Binding and unbinding kinetics of DLC1 to talin R8.

Concentration DLC1 (nM)	10	100	1000
Binding rate $x10^3$ (s^{-1})	5.9 ± 0.7	7 ± 1	6 ± 2
Unbinding rate $x10^3$ (s^{-1})	4 ± 1	6 ± 2	10 ± 1
Number of events, *N*	50	39	29

Supplementary Figures:

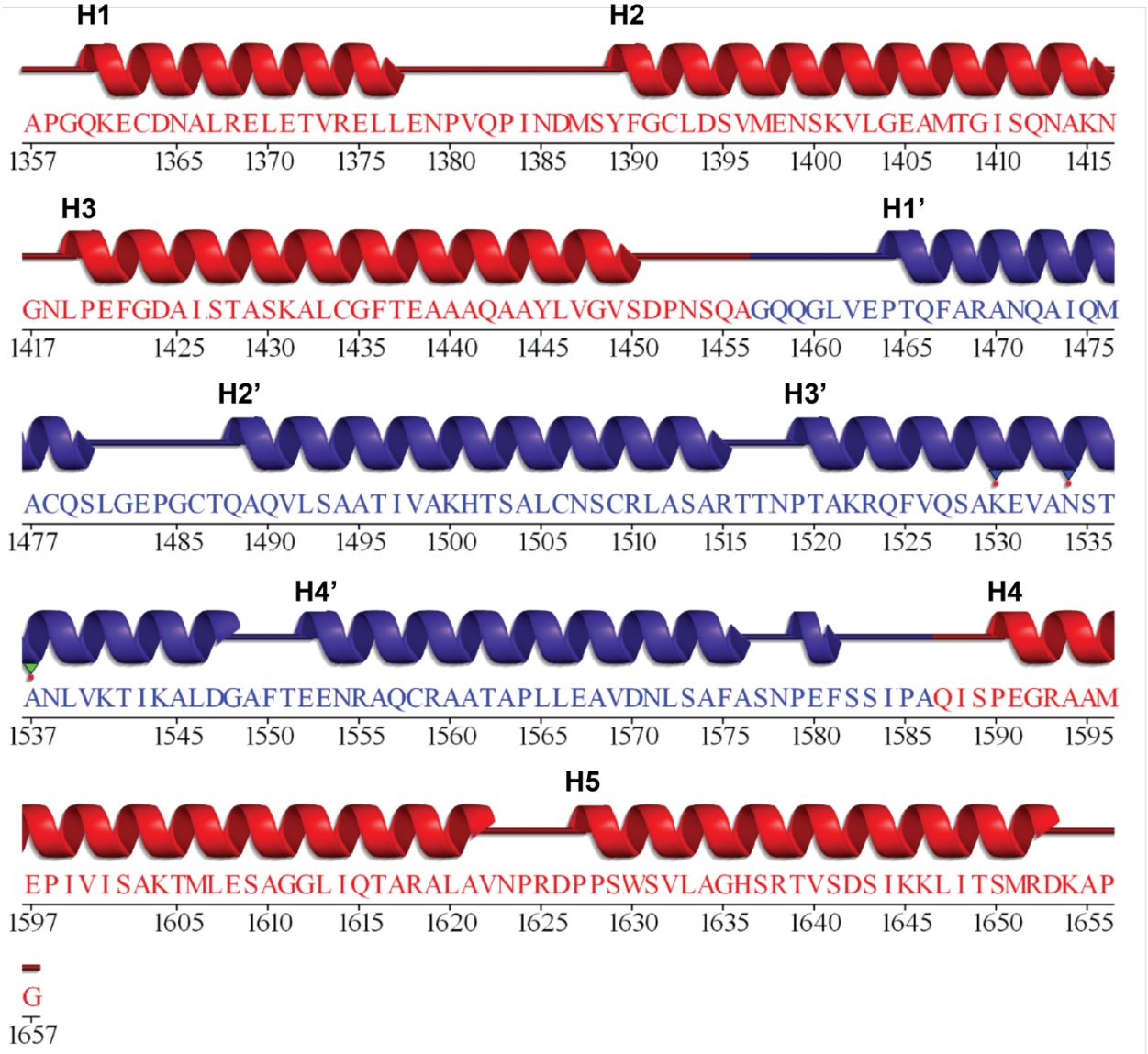

Supplementary Figure 1. Structural classification of talin R7R8 domain. Structural classification generated using http://www.ebi.ac.uk/ and the crystal structure with pdb code 4w8p. The color code shows R7 and R8 portions with red and blue, respectively. The helices of R7 are labeled from H1 to H5, while the helices of R8 are labeled with H1' to H4'.

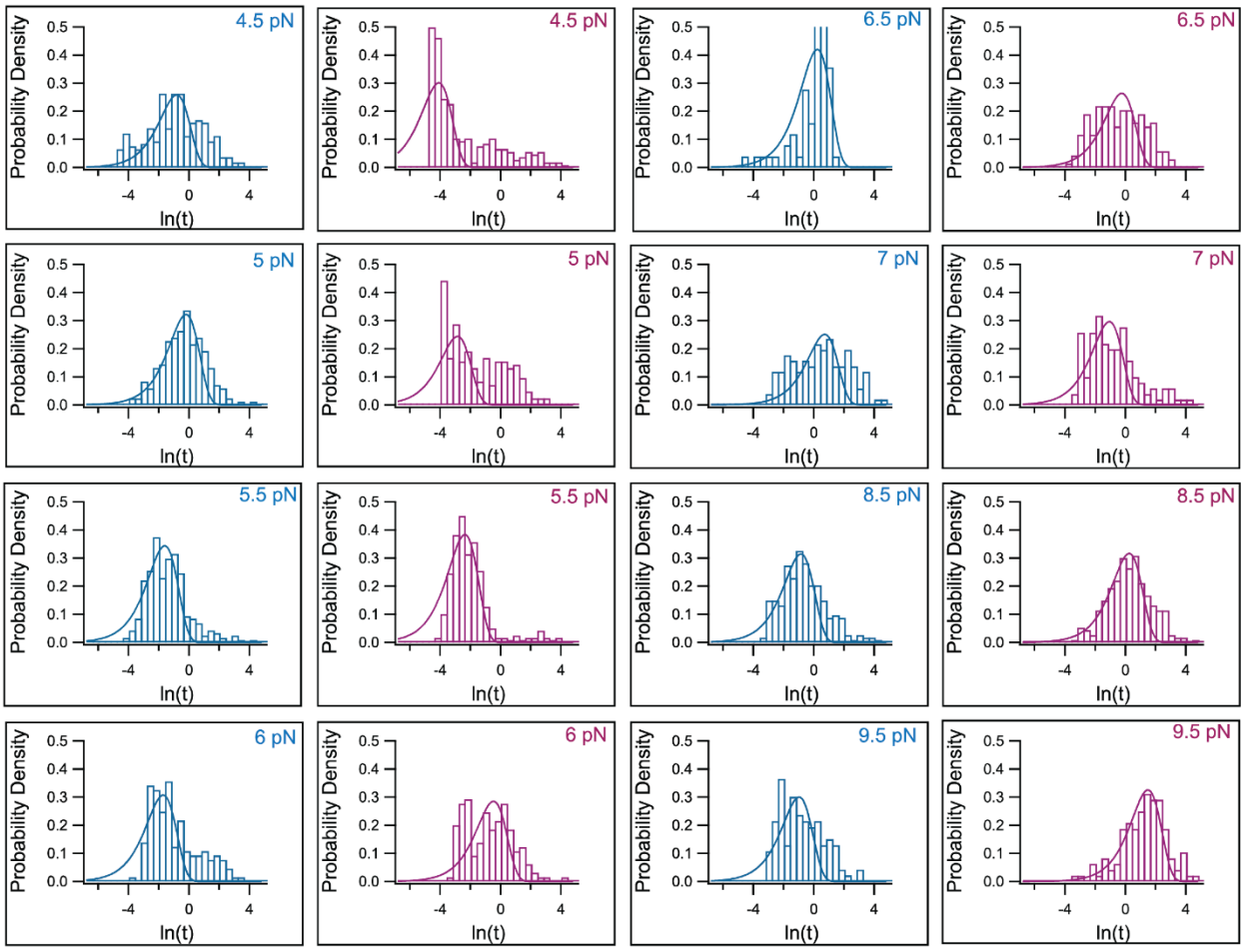

Supplementary Figure 2. Histograms of natural logarithm of dwell time as a function of probability density at various forces for talin R8 domain. The force varies in physiological range from 4.5 pN to 9.5 pN. Magenta histograms are obtained for the folded states and blue histograms are for the unfolded states.

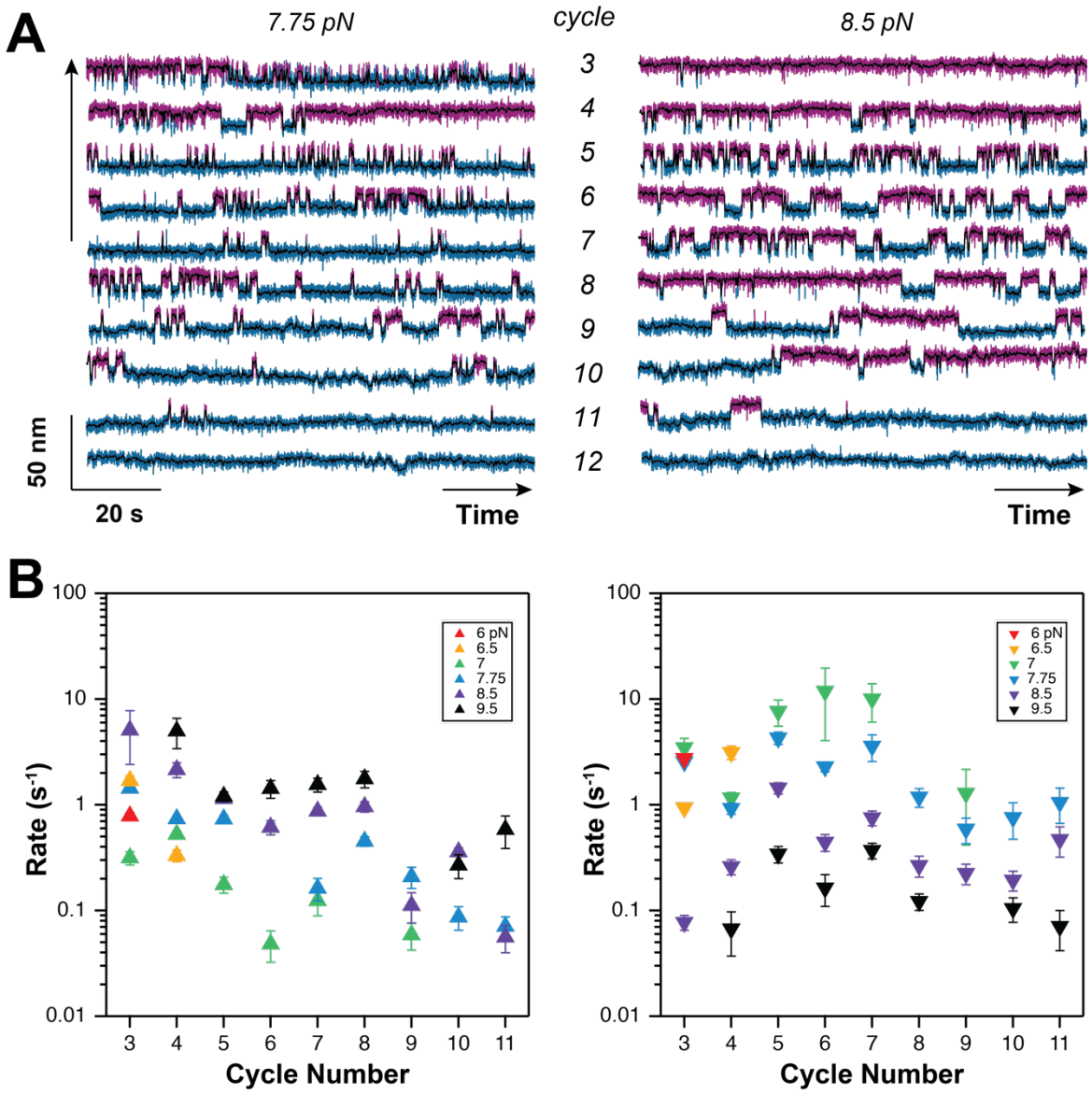

Supplementary Figure 3: History dependent behavior on unfolding and refolding equilibrium of R8 domain. A) Representative traces of unfolding and refolding transition of R8 at a given force. (left) The traces from top to bottom represents the same molecule exposed to 7.75 pN at different force cycles; (right) similar traces obtained from the same molecule at 8.5 pN. Magenta color represents the unfolded states and blue represents the folded states. All traces presented shown above were obtained from the same molecule. B) Unfolding and refolding rates at various forces as a function of cycle number, collected from traces with more than 5 events.

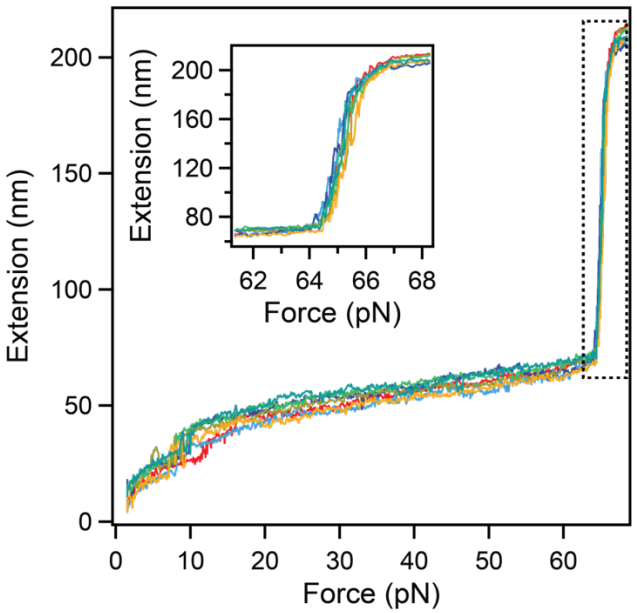

Supplementary Figure 4. Comparison between fingerprint cycles for trace in Fig.3. Molecular extension vs applied force. Inset: measured extension vs force for the overstretching DNA transition showing no variance in the position of the overstretching transition and representing a second indirect measurement for potential force drift. Dotted box represents the magnified view from inset.

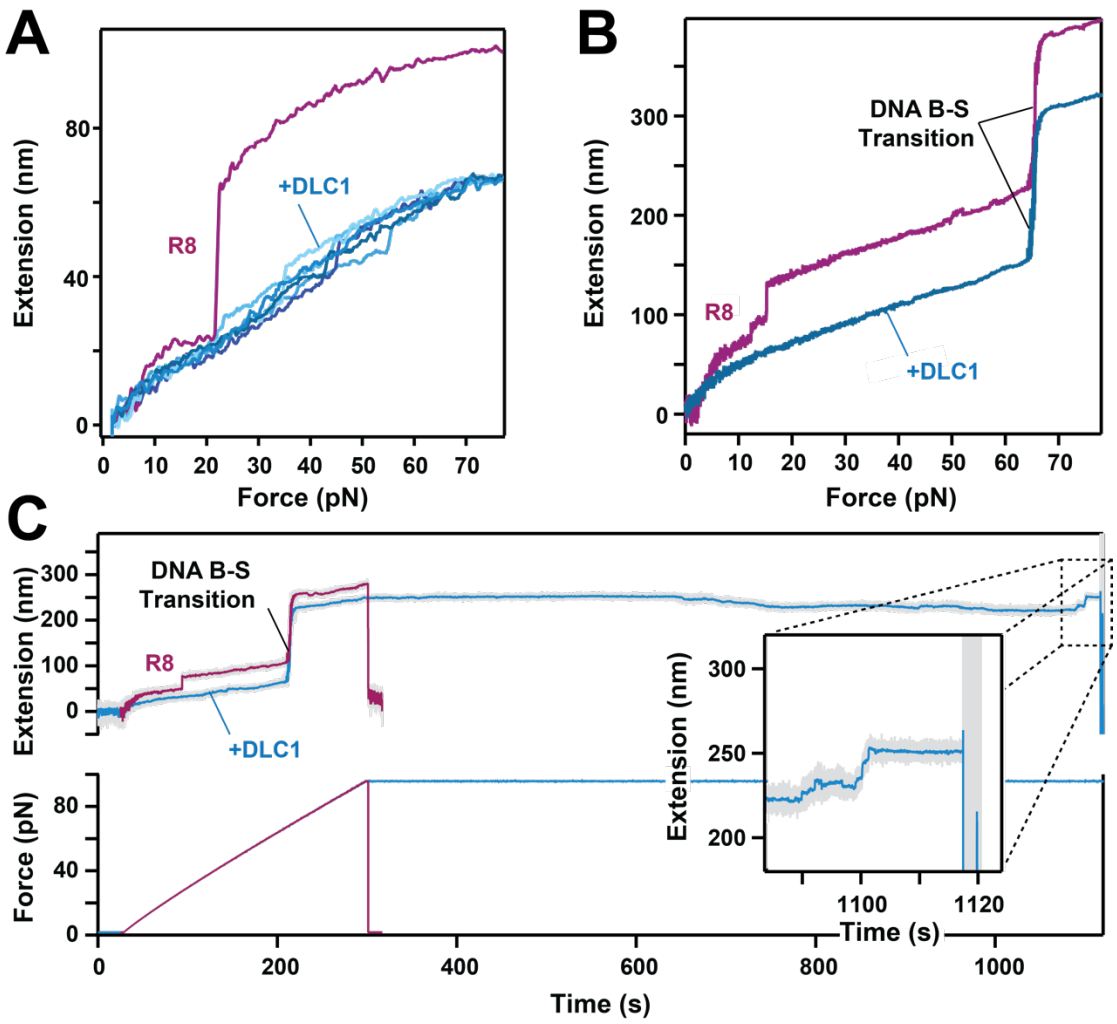

Supplementary Figure 5: Force extension traces of the same talin R8 molecule in the absence and presence of DLC1 ligand. A) Traces of the R8 construct before addition of DLC1 (purple) and after addition of DLC1. No unfolding fingerprint was measured during all the cycles after addition of DLC1. DLC1 concentration:1.2 μM; pulling rate: 15.5 pN/s. B) Traces of the R8-DNA construct before and after addition DLC1 (purple and magenta, respectively). Both traces show the DNA overstretching transition. DLC1 concentration: 14 μM; pulling rate: 0.33 pN/s. C) Extension and force as a function of time for the same R8-DNA molecule in the absence and presence of DLC1. Inset: rupture steps which we typically measure before the detachment of the di-biotin end of the molecule. DLC1 concentration:10 nM. All traces were filtered with a 50 box filter. Grey trace in panel C represents raw data.

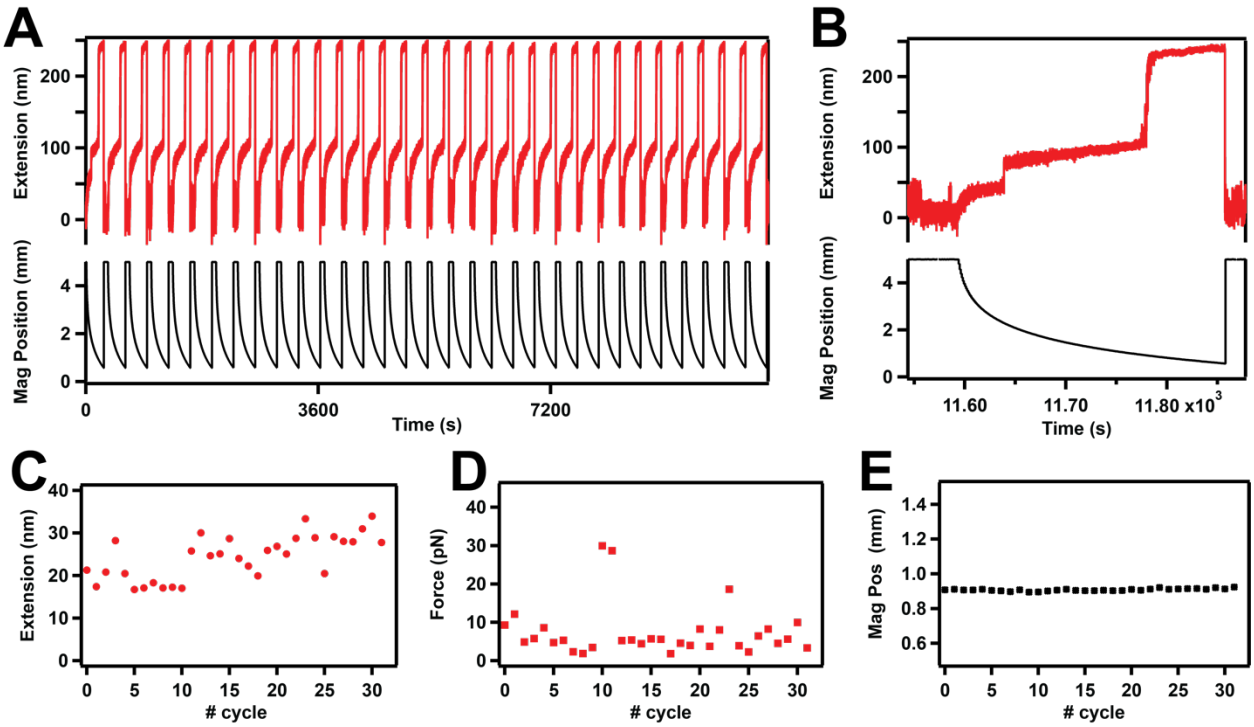

Supplementary Figure 6: Assessment of potential instrumental drift in applied force using molecular fingerprints. A) Single molecule magnetic tweezers trace where a R8-DNA construct is cycled between a linear increase in force with time, to unfold the talin domain and sample the DNA overstretching transition, followed by a quench in force, which allows for the refolding of the protein. B) Zoom-in of one of the cycles. C) Variation of unfolding extension of R8 as a function of cycle number. D) Variation in the measured unfolding force for R8 as a function of cycle number. E) Change in the measured position of the DNA overstretching transition with cycle number. A significant change would be indicative of instrumental drift over time.

REFERENCES AND NOTES

1. M. Mora, A. Stannard, S. Garcia-Manyes, The nanomechanics of individual proteins. *Chem. Soc. Rev.* **49**, 6816–6832 (2020).

2. R. Berkovich, V. I. Fernandez, G. Stirnemann, J. Valle-Orero, J. M. Fernandez, Segmentation and the entropic elasticity of modular proteins. *J. Phys. Chem. Lett.* **9**, 4707–4713 (2018).

3. K. C. Neuman, A. Nagy, Single-molecule force spectroscopy: Optical tweezers, magnetic tweezers and atomic force microscopy. *Nat. Methods* **5**, 491–505 (2008).

4. I. Popa, J. A. Rivas-Pardo, E. C. Eckels, D. J. Echelman, C. L. Badilla, J. Valle-Orero, J. M. Fernandez, A halotag anchored ruler for week-long studies of protein dynamics. *J. Am. Chem. Soc.* **138**, 10546–10553 (2016).

5. A. W. Haining, T. J. Lieberthal, A. Del Rio Hernandez, Talin: A mechanosensitive molecule in health and disease. *FASEB J.* **30**, 2073–2085 (2016).

6. M. Yao, B. T. Goult, B. Klapholz, X. Hu, C. P. Toseland, Y. Guo, P. Cong, M. P. Sheetz, J. Yan, The mechanical response of talin. *Nat. Commun.* **7**, 11966 (2016).

7. A. del Rio, R. Perez-Jimenez, R. Liu, P. Roca-Cusachs, J. M. Fernandez, M. P. Sheetz, Stretching single talin rod molecules activates vinculin binding. *Science* **323**, 638–641 (2009).

8. R. Tapia-Rojo, A. Alonso-Caballero, J. M. Fernandez, Direct observation of a coil-to-helix contraction triggered by vinculin binding to talin. *Sci. Adv.* **6**, eaaz4707 (2020).

9. C. Kluger, L. Braun, S. M. Sedlak, D. A. Pippig, M. S. Bauer, K. Miller, L. F. Milles, H. E. Gaub, V. Vogel, Different vinculin binding sites use the same mechanism to regulate directional force transduction. *Biophys. J.* **118**, 1344–1356 (2020).

10. A. R. Gingras, N. Bate, B. T. Goult, B. Patel, P. M. Kopp, J. Emsley, I. L. Barsukov, G. C. K. Roberts, D. R. Critchley, Central region of talin has a unique fold that binds vinculin and actin. *J. Biol. Chem.* **285**, 29577–29587 (2010).

11. N. Dahal, J. Nowitzke, A. Eis, I. Popa, Binding-induced stabilization measured on the same molecular protein substrate using single-molecule magnetic tweezers and heterocovalent attachments. *J. Phys. Chem. B* **124**, 3283–3290 (2020).

12. J. Valle-Orero, J. A. Rivas-Pardo, I. Popa, Multidomain proteins under force. *Nanotechnology* **28**, 174003 (2017).

13. S. R. Ainavarapu, J. Brujic, H. H. Huang, A. P. Wiita, H. Lu, L. Li, K. A. Walther, M. Carrion-Vazquez, H. Li, J. M. Fernandez, Contour length and refolding rate of a small protein controlled by engineered disulfide bonds. *Biophys. J.* **92**, 225–233 (2007).

14. A. W. M. Haining, R. Rahikainen, E. Cortes, D. Lachowski, A. Rice, M. von Essen, V. P. Hytonen, A. D. Hernandez, Mechanotransduction in talin through the interaction of the R8 domain with DLC1. *PLOS Biol.* **16**, e2005599 (2018).

15. R. Tapia-Rojo, E. C. Eckels, J. M. Fernandez, Ephemeral states in protein folding under force captured with a magnetic tweezers design. *Proc. Natl. Acad. Sci. U.S.A.* **116**, 7873–7878 (2019).

16. R. Tapia-Rojo, A. Alonso-Caballero, J. M. Fernandez, Talin folding as the tuning fork of cellular mechanotransduction. *Proc. Natl. Acad. Sci. U.S.A.* **117**, 21346–21353 (2020).

17. R. Berkovich, S. Garcia-Manyes, M. Urbakh, J. Klafter, J. M. Fernandez, Collapse dynamics of single proteins extended by force. *Biophys. J.* **98**, 2692–2701 (2010).

18. T. Y. Kim, K. D. Healy, C. J. Der, N. Sciaky, Y. J. Bang, R. L. Juliano, Effects of structure of Rho GTPase-activating protein DLC-1 on cell morphology and migration. *J. Biol. Chem.* **283**, 32762–32770 (2008).

19. T. Zacharchenko, X. Qian, B. T. Goult, D. Jethwa, T. B. Almeida, C. Ballestrem, D. R. Critchley, D. R. Lowy, I. L. Barsukov, LD motif recognition by talin: Structure of the talin-DLC1 complex. *Structure* **24**, 1130–1141 (2016).

20. Y. Cao, M. M. Balamurali, D. Sharma, H. Li, A functional single-molecule binding assay via force spectroscopy. *Proc. Natl. Acad. Sci. U.S.A.* **104**, 15677–15681 (2007).

21. J. Valle-Orero, J. A. Rivas-Pardo, R. Tapia-Rojo, I. Popa, D. J. Echelman, S. Haldar, J. M. Fernandez, Mechanical deformation accelerates protein ageing. *Angew. Chem. Int. Ed. Engl.* **56**, 9741–9746 (2017).

22. B. Klapholz, N. H. Brown, Talin—The master of integrin adhesions. *J. Cell Sci.* **130**, 2435–2446 (2017).

23. K. Austen, P. Ringer, A. Mehlich, A. Chrostek-Grashoff, C. Kluger, C. Klingner, B. Sabass, R. Zent, M. Rief, C. Grashoff, Extracellular rigidity sensing by talin isoform-specific mechanical linkages. *Nat. Cell Biol.* **17**, 1597–1606 (2015).

24. F. Margadant, L. L. Chew, X. Hu, H. Yu, N. Bate, X. Zhang, M. Sheetz, Mechanotransduction in vivo by repeated talin stretch-relaxation events depends upon vinculin. *PLoS Biol.* **9**, e1001223 (2011).

25. A. W. M. Haining, M. von Essen, S. J. Attwood, V. P. Hytonen, A. D. Hernandez, All subdomains of the talin rod are mechanically vulnerable and may contribute to cellular mechanosensing. *ACS Nano* **10**, 6648–6658 (2016).

26. I. Popa, J. H. Gutzman, The extracellular matrix–myosin pathway in mechanotransduction: From molecule to tissue. *Emerg. Top. Life Sci.* **2**, 727–737 (2018).

27. S. Sharma, S. Subramani, I. Popa, Does protein unfolding play a functional role in vivo? *FEBS J.* **288**, 1742–1758 (2021).

28. C. M. Wong, J. M. Lee, Y. P. Ching, D. Y. Jin, I. O. Ng, Genetic and epigenetic alterations of DLC-1 gene in hepatocellular carcinoma. *Cancer Res.* **63**, 7646–7651 (2003).

29. V. Ullmannova, N. C. Popescu, Expression profile of the tumor suppressor genes DLC-1 and DLC-2 in solid tumors. *Int. J. Oncol.* **29**, 1127–1132 (2006).

30. S. M. Sedlak, L. C. Schendel, H. E. Gaub, R. C. Bernardi, Streptavidin/biotin: Tethering geometry defines unbinding mechanics. *Sci. Adv.* **6**, eaay5999 (2020).

31. S. Gruber, A. Lof, S. M. Sedlak, M. Benoit, H. E. Gaub, J. Lipfert, Designed anchoring geometries determine lifetimes of biotin-streptavidin bonds under constant load and enable ultra-stable coupling. *Nanoscale* **12**, 21131–21137 (2020).

32. Z. N. Scholl, W. Yang, P. E. Marszalek, Chaperones rescue luciferase folding by separating its domains. *J. Biol. Chem.* **289**, 28607–28618 (2014).

33. K. Liu, X. Chen, C. M. Kaiser, Energetic dependencies dictate folding mechanism in a complex protein. *Proc. Natl. Acad. Sci. U.S.A.* **116**, 25641–25648 (2019).

34. M. Baiesi, E. Orlandini, F. Seno, A. Trovato, Sequence and structural patterns detected in entangled proteins reveal the importance of co-translational folding. *Sci. Rep.* **9**, 8426 (2019).

35. D. A. Nissley, Y. Jiang, F. Trovato, I. Sitarik, K. B. Narayan, P. Yo, Y. Xia, S.D. Fried, E. P. O'Brien, Universal protein misfolding intermediates can bypass the proteostasis network and remain soluble and non-functional. *Nat. Commun.* **13**, 3081 (2022).

36. C. A. Waudby, C. M. Dobson, J. Christodoulou, Nature and regulation of protein folding on the ribosome. *Trends Biochem. Sci.* **44**, 914–926 (2019).

37. R. Tapia-Rojo, A. Alonso-Caballero, C. L. Badilla, J. M. Fernandez, Identical sequences, different behaviors: Protein diversity captured at the single-molecule level. *bioRxiv*, 2021.02.24.432730 (2021).

38. S. Garcia-Manyes, J. Liang, R. Szoszkiewicz, T. L. Kuo, J. M. Fernandez, Force-activated reactivity switch in a bimolecular chemical reaction. *Nat. Chem.* **1**, 236–242 (2009).

39. M. E. Durkin, M. R. Avner, C. G. Huh, B. Z. Yuan, S. S. Thorgeirsson, N. C. Popescu, DLC-1, a Rho GTPase-activating protein with tumor suppressor function, is essential for embryonic development. *FEBS Lett.* **579**, 1191–1196 (2005).

40. Y. C. Liao, Y. P. Shih, S. H. Lo, Mutations in the focal adhesion targeting region of deleted in liver cancer-1 attenuate their expression and function. *Cancer Res.* **68**, 7718–7722 (2008).

41. T. A. Springer, M. L. Dustin, Integrin inside-out signaling and the immunological synapse. *Curr. Opin. Cell Biol.* **24**, 107–115 (2012).

42. M. Yao, B. T. Goult, H. Chen, P. Cong, M. P. Sheetz, J. Yan, Mechanical activation of vinculin binding to talin locks talin in an unfolded conformation. *Sci. Rep.* **4**, 4610 (2014).

43. A. Stannard, M. Mora, A. E. M. Beedle, M. Castro-Lopez, S. Board, S. Garcia-Manyes, Molecular fluctuations as a ruler of force-induced protein conformations. *Nano Lett.* **21**, 2953–2961 (2021).

44. D. Dedden, S. Schumacher, C. F. Kelley, M. Zacharias, C. Biertumpfel, R. Fassler, N. Mizuno, The architecture of Talin1 reveals an autoinhibition mechanism. *Cell* **179**, 120–131.e13 (2019).

45. Y. C. Chang, H. Zhang, J. Franco-Barraza, M. L. Brennan, T. Patel, E. Cukierman, J. Wu, Structural and mechanistic insights into the recruitment of talin by RIAM in integrin signaling. *Structure* **22**, 1810–1820 (2014).

46. B. P. Bouchet, R. E. Gough, Y. C. Ammon, D. van de Willige, H. Post, G. Jacquemet, A. M. Altelaar, A. J. Heck, B. T. Goult, A. Akhmanova, Talin-KANK1 interaction controls the recruitment of cortical microtubule stabilizing complexes to focal adhesions. *eLife* **5**, e18124 (2016).

47. M. R. Stoneman, G. Biener, R. J. Ward, J. D. Pediani, D. Badu, A. Eis, I. Popa, G. Milligan, V. Raicu, A general method to quantify ligand-driven oligomerization from fluorescence-based images. *Nat. Methods* **16**, 493–496 (2019).

48. Y. Zhang, J. Jiao, A. A. Rebane, Hidden Markov modeling with detailed balance and its application to single protein folding. *Biophys. J.* **111**, 2110–2124 (2016).

49. A. P. Wiita, R. Perez-Jimenez, K. A. Walther, F. Grater, B. J. Berne, A. Holmgren, J. M. Sanchez-Ruiz, J. M. Fernandez, Probing the chemistry of thioredoxin catalysis with force. *Nature* **450**, 124–127 (2007).

50. R. B. Khan, B. T. Goult, Adhesions assemble!-autoinhibition as a major regulatory mechanism of integrin-mediated adhesion. *Front. Mol. Biosci.* **6**, 144 (2019).

51. M. D. Bass, B. Patel, I. G. Barsukov, I. J. Fillingham, R. Mason, B. J. Smith, C. R. Bagshaw, D. R. Critchley, Further characterization of the interaction between the cytoskeletal proteins talin and vinculin. *Biochem. J.* **362**, 761–768 (2002).

52. H. Chen, D. M. Choudhury, S. W. Craig, Coincidence of actin filaments and talin is required to activate vinculin. *J. Biol. Chem.* **281**, 40389–40398 (2006).

53. P. W. Miller, S. Pokutta, J. M. Mitchell, J. V. Chodaparambil, D. N. Clarke, W. J. Nelson, W. I. Weis, S. A. Nichols, Analysis of a vinculin homolog in a sponge (phylum Porifera) reveals that vertebrate-like cell adhesions emerged early in animal evolution. *J. Biol. Chem.* **293**, 11674–11686 (2018).

54. B. T. Goult, T. Zacharchenko, N. Bate, R. Tsang, F. Hey, A. R. Gingras, P. R. Elliott, G. C. K. Roberts, C. Ballestrem, D. R. Critchley, I. L. Barsukov, RIAM and vinculin binding to talin are mutually exclusive and regulate adhesion assembly and turnover. *J. Biol. Chem.* **288**, 8238–8249 (2013).